Supporting Information for

# Fate and transformation of graphene oxide in estuarine and marine waters

Adeyemi S. Adeleye[a, 1,*], Kay T. Ho[b], Min Zhang[c], Yao Li[c], and Robert M. Burgess[b]

[a] *National Research Council Research Associate, US Environmental Protection Agency, Atlantic Ecology Division, 27 Tarzwell Dr., Narragansett, RI 02882, USA*

[b] *US Environmental Protection Agency, Atlantic Ecology Division, 27 Tarzwell Dr., Narragansett, RI 02882, USA*

[c] *Key Laboratory of Pollution Processes and Environmental Criteria/Tianjin Key Laboratory of Environmental Remediation and Pollution Control, Nankai University, Tong Yan Road 38, Tianjin 300350, China*

*Corresponding author: A.S.A. (Phone) 949-824-5819; (E-mail) adeyemi.adeleye@uci.edu

[1] Current address: Department of Civil and Environmental Engineering, University of California, Irvine, CA 92697, United States

Number of pages: 25

Figures: 15

Tables: 3

S1. **GO characterization**

Few-layer (2-4 layers) graphene oxide (GO) was obtained as a dry powder from Cheap Tubes (Cambridgeport, VT) and used as received without further modification. According to the manufacturer the GO was synthesized by a modified hummer's method, and it had a purity of 99%. The GO powder was characterized via X-ray photoelectron spectroscopy (XPS; PHI 5000 VersaProbe, ULVAC-PHI, Japan), atomic force microscopy (AFM; Bruker Dimension Icon, Billerica, MA), Raman spectroscopy (RTS-HiR-AM Raman spectrometer, TEO, China), transmission electron microscopy (TEM; JEOL JEM-2800, Japan), X-ray diffraction (XRD; Ulitma IV X-ray diffractometer, Rigaku Corporation, Japan), and Fourier transform infrared spectroscopy (FTIR; Bruker TENSOR 27, Germany). A ZetaPALS Analyzer (Brookhaven Instruments, Holtsville, NY) was used to determine the hydrodynamic diameter and zeta (ζ) potential of the GO in deionized (DI) water (≥ 18.2 MΩ.cm, Milli-Q Element, Millipore, Billerica, MA) and seawater via dynamic light scattering (DLS) and phase analysis light scattering (PALS) techniques, respectively, using well-established methods.[1, 2] For DLS analysis the intensity of scattered light was measured at 90°, and an autocorrelation function was allowed to accumulate for 3 min per measurement. Each ζ potential measurement was an average of 10 runs made up of 30 cycles for the measurements in DI water or 1 run made up of 100 cycles for measurements in seawater. Samples prepared in DI water were kept at pH 7 using 0.5 mM phosphate buffer; and ionic strength was adjusted to 1 mM NaCl for the ζ potential measurements in DI water.

**S2. GO stock preparation**

A fresh GO stock suspension in DI water was prepared for each experiment and analysis. To prepare the stock, a known amount of GO powder was suspended in freshly-collected DI water to achieve a GO concentration of 200 mg/L. The stock suspension was dispersed via probe sonication using a tapered microtip connected to a Sonifier SFX 250 (Branson Ultrasonics, Danbury, CT). A sonication time of 1 h was used, which was made up of cycles of 30 s on and 30 s off intervals (hence, actual sonication time was 30 min). The GO suspensions were kept in an ice-bath during probe sonication to minimize mechanical damage.

**S3. Natural organic materials (NOM)**

Two representatives of NOM—humic acid (HA) and soluble extracellular polymeric substances (EPS)—were used for this study. HA, obtained as a sodium salt from Sigma Aldrich (St. Louis, MO), was used to represent commercially available NOM. Stocks of HA were prepared in 0, 1, and 30 ‰ media. Preliminary tests showed that some HA materials agglomerated and settled out of the 1 and 30 ‰ media. To avoid this NOM instability in saline waters from interfering with GO agglomeration and sedimentation studies, 500 mg/L suspensions of HA were prepared directly in 1 and 30 ‰ media using the following procedures. The suspensions were mixed with a magnetic stir bars for 6 weeks, followed by sonication in water bath for 6 h (Branson 1210). The mixed suspensions were then allowed to settle over a period of 7 weeks. The supernatant, which contained stable NOM fractions, was carefully decanted and filtered through Nalgene 0.2 µm aPES filter units (Thermo Scientific, Waltham, MA).

EPS represents the exudates from marine microorganisms, which are abundant in natural waters. The EPS used in this study was extracted from a marine phytoplankton, *Tetraselmis* sp., as described in previous studies.[3-5] The phytoplankton was maintained in f/2 media (Kent algal media A and B) made with autoclaved 0.2 µm-filtered natural seawater collected from Narragansett Bay, RI. Algae was incubated under cool white fluorescent lights (18:6 light:dark) at 20 °C with aeration. Cell densities were measured using a fluorometer (Trilogy, Turner Designs), which was converted to cell numbers using a standard curve based on counts performed with a hemacytometer (Reichert, Buffalo NY). When the cells reached the stationary growth phase they were removed from the growth media via centrifugation (15 min at 2500 *g*, Hermle Z206A, Germany). The supernatant was then filtered (0.22 µm aPES filter, Thermo Fisher Scientific) to completely remove cells and large macromolecules. The filtrate contained the EPS, which was precipitated using cold ethanol (2:1 ethanol:media) and kept at 4 °C for 24 h. The precipitated EPS was then separated via centrifugation (10 min at 6000 *g*). To remove the residual salts from the growth medium and low molecular-weight metabolites, EPS was dialyzed against DI water at 4 °C using 3500 Da MWCO Spectra/Por 3 regenerated cellulose dialysis tubing (Spectrum Laboratories, Racho Dominguez, CA), which had been treated with Spectrum Laboratories heavy metal cleaning solution. The dialysis DI water was renewed twice daily until the conductivity (YSI 556 MPS, Yellow Springs, OH) of the dialyzate did not change following

three consecutive renewals (about 7-8 days). The dialyzed EPS was stored in the dark at 4 °C until use.

Both HA and EPS were characterized by measuring carbohydrate and protein concentrations using anthrone-sulfuric acid method and modified Bradford protein assay, respectively. Dissolved organic carbon (DOC) was determined using a Shimadzu TOC-V CPH TOC analyzer. FTIR spectra of EPS and HA were obtained using a Thermo Nicolet iS50 spectrometer with a diamond ATR crystal. Interferograms were obtained by taking 256 scans with a resolution of 2 $cm^{-1}$.

**S4. Sedimentation kinetics**

Sedimentation of GO was determined at a range of media salinity (0 - 50 ‰), NOM concentrations (1-10 mg/L DOC) and GO state (pristine and aged). For each study, 3-4 replicates were used per treatment. Pre-determined amounts of GO stock, natural brine, DI water, and NOM (when needed) were added together in KIMAX borosilicate culture tubes to achieve a final volume of 50 mL. For all studies, a final GO concentration of 10 mg/L was used to ensure strong signal was obtained from the analytical technique used, UV-Vis spectroscopy (Biotek Synergy HTX multi-mode reader).[6] At the start of the sedimentation experiment, we ensured that the 50 mL GO suspension was homogeneous by a combination of thorough shaking and probe sonication (10 s). As a result, the initial sample was from an evenly distributed sample. Sedimentation experiments were carried out for 28 days, and sampling was performed at 0, 2, 4, 6 h, and 1, 2, 3, 7, 14, 21, and 28 days. For sampling, a 0.5 mL aliquot was removed from a point 3 cm below the original meniscus of each suspension throughout the study (so we could determine the sedimentation velocity more accurately by having a fixed reference settling height) and transferred into holding disposable test tubes covered with parafilm to prevent contamination. From the 0.5 mL aliquot, two transfers, 0.2 mL each, were then made into wells of a UV flat bottom microplate (Themo Electron, Weaverville, NC) and the absorbance of each transfer was determined at 230 nm.[7] For the 28-d period, sample tubes containing GO suspensions were kept at room temperature (20-22 °C) under cool white fluorescent lights (16:8 light:dark cycle) The light source were two 40W Philips F40T12/CW Supreme/ALTO lamps in fixtures, with a total irradiance of 16-25 μmol/$m^2$-s. To account for the absorbance due to diluted

bring and NOM we also had control samples (n = 3 or 4) which were the same composition as the experimental samples except GO. The control samples were measured like the real samples and the average absorbance of the controls was subtracted from the average absorbance of experimental samples. Since absorbance is directly correlated with GO concentration, it was used as a proxy for GO concentration without any conversion. A semi-empirical model (Eq. S1) was to describe the sedimentation of GO as a function of time.[8]

$$a_t = (a_0 - a_f)e^{-\left(\frac{V_s}{h}+k_{diss}\right)t} + a_f \qquad \text{(S1)}$$

where $a_0$ is the initial absorbance of GO, $a_f$ is the absorbance after infinite time based on data measured at 28 d. $V_s$ (m/d) is the sedimentation rate, h is the sedimentation length (0.03 m in this study), $k_{diss}$ is the dissolution rate constant, which is (0/d) for GO; and $t$ is the elapsed time (d).

**S5. Agglomeration kinetics**

The agglomeration of GO was determined at a range of media salinity (0 - 30 ‰), NOM concentrations (1-10 mg/L DOC) and GO state (pristine and aged). Since the saline waters were prepared by mixing known volumes of natural brine and DI water, the amount of all the ions present at each salinity was proportional. This is analogous to what is obtainable when determining the critical coagulation concentration (CCC) of simple salts for nanomaterials. Thus, the agglomeration kinetics of GO was studied at increasing salinity to determine if the typical reaction-limited (RLCA) and diffusion-limited (DLCA) clustering agglomeration regimes will be identified. As shown in Eq. S2, the initial agglomeration rate constant (*k*) reflects doublet formation and is proportional to the initial rate of increase in the intensity-weighted hydrodynamic size, $a_h(t)$, with time, t, and the inverse of initial number concentration of nanoparticles, $N_0$:[2, 5, 9]

$$k \propto \frac{1}{N_0}\left[\frac{da_h(t)}{dt}\right]_{t\to 0} \qquad \text{(S2)}$$

Attachment efficiencies ($\alpha$) of GO at different salinities were calculated by normalizing the measured *k* of a given salinity by the diffusion-limited agglomeration rate constant $(k)_{fav}$ determined in highly favorable agglomeration conditions (Eq. S3):

$$\alpha = \frac{\left[\frac{da_h(t)}{dt}\right]_{t\to 0}}{\left[\frac{da_h(t)}{dt}\right]_{t\to 0,fav}} \quad \text{(S3)}$$

Agglomeration kinetics were monitored using the ZetaPALS immediately after adding appropriate amounts of GO stock, natural brine, DI water, and NOM (if needed). Data were collected until a 50% increase in the initial hydrodynamic size was observed.

Table S1. A summary of the high resolution XPS analysis of the C 1s peak of GO suspended in 0 and 30 ‰, and irradiated using a solar simulator for 6, 12 or 24 h.

| Sample | C 1s | | | | Total C (Atomic %) | Total O (Atomic %) | Total Cl (Atomic %) | Total Na (Atomic %) | C/O ratio |
|---|---|---|---|---|---|---|---|---|---|
| | C-C/C=C | C-OH/ C-O-C | C=O | O-C=O | | | | | |
| **0 ‰, 6 h** | 58.57 | 33.68 | 2.00 | 5.57 | 75.69 | 24.31 | 0 | 0 | 3.11 |
| **30 ‰, 6 h** | 62.81 | 28.82 | 3.56 | 4.81 | 71.65 | 25.73 | 0.90 | 1.71 | 2.78 |
| **0 ‰, 12 h** | 63.63 | 28.39 | 2.77 | 5.21 | 77.47 | 22.53 | 0 | 0 | 3.44 |
| **30 ‰, 12 h** | 63.30 | 27.81 | 4.47 | 4.43 | 71.98 | 24.84 | 1.12 | 2.06 | 2.90 |
| **0 ‰, 24 h** | 67.09 | 23.50 | 3.44 | 5.97 | 78.63 | 21.37 | 0 | 0 | 3.62 |
| **30 ‰, 24 h** | 64.73 | 25.75 | 4.28 | 5.24 | 74.26 | 22.89 | 0.91 | 1.94 | 3.24 |

Table S2. Band assignment of EPS isolated from *Tetraselmis sp*.[4, 10-12]

| **Wavenumber ($cm^{-1}$)** | **Band assignment** |
|---|---|
| 576 | C=O out-of-plane bend in amides of proteins |
| 767 | $NH_2$ wag in primary amines of proteins |
| 926 | P-O-C antisym stretch in organophosphorus compounds |
| 1028 | C-O stretch of phosphorylated proteins or polysaccharides |
| 1061 | C-O, C-O-C stretch of polysaccharides |
| 1153 | C-O stretching of polysaccharides or amino acids |
| 1214 | P=O stretch of phospholipids or nucleic acids |
| 1376 | C-O sym stretching of carboxylic acid salts |
| 1413 | $COO^-$ stretching of carboxylic acids in amino acids (amide II) |
| 1619 | $NH_2$ deformation in primary amines of proteins, $COO^-$ antisym stretching of carboxylic acid salts |
| 2923, 2949 | CH antisym and sym stretch of lipids |
| 3367 | OH stretching, $NH_2$ antisym stretching in amides of proteins |

Table S3. Band assignment of humic acid sodium salt obtained from Sigma Aldrich.[4, 10-12]

| **Wavenumber ($cm^{-1}$)** | **Band assignment** |
|---|---|
| 464 | C-N-C bend in amines or C-C=O bend in carboxylic acids of proteins |
| 532 | C=O out-of-plane bend in amides of proteins |
| 685 | C=O bend carboxylic acids of proteins |
| 778 | $NH_2$ wag in primary amines of proteins |
| 912 | P-O-C antisym stretch in organophosphorus compounds |
| 1007 | C-O stretch of polysaccharides |
| 1030 | C-O stretch of polysaccharides |
| 1087 | C-O, C-O-C stretch of polysaccharides |
| 1376 | $COO^-$ sym stretching of carboxylic acid salts |
| 1573 | $NH_2$ deformation in primary amines of proteins, $COO^-$ antisym stretching of carboxylic acid salts |
| 2924 | CH antisym and sym stretch of lipids |
| 3381 | OH stretching, $NH_2$ antisym stretching in amides of proteins |

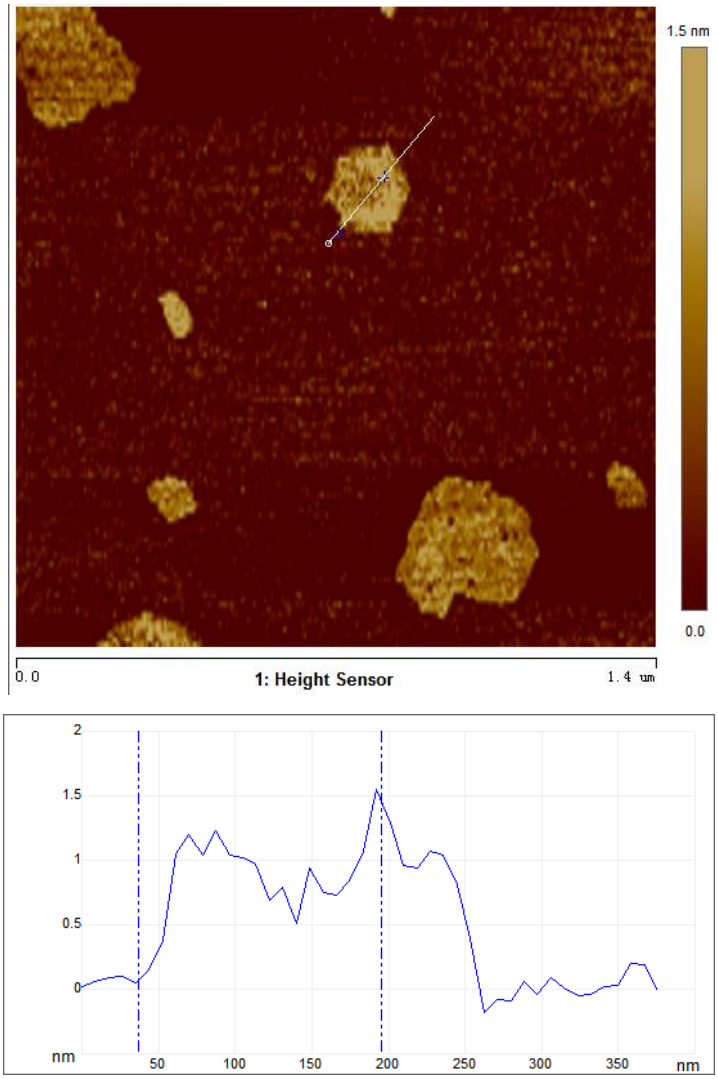


Figure S1. The atomic force micrograph of GO used in this study. The height profile of the cross section of one GO particle (designated by white line on the micrograph) is shown below, demonstrating GO thickness of 0.5 – 1.5 nm.

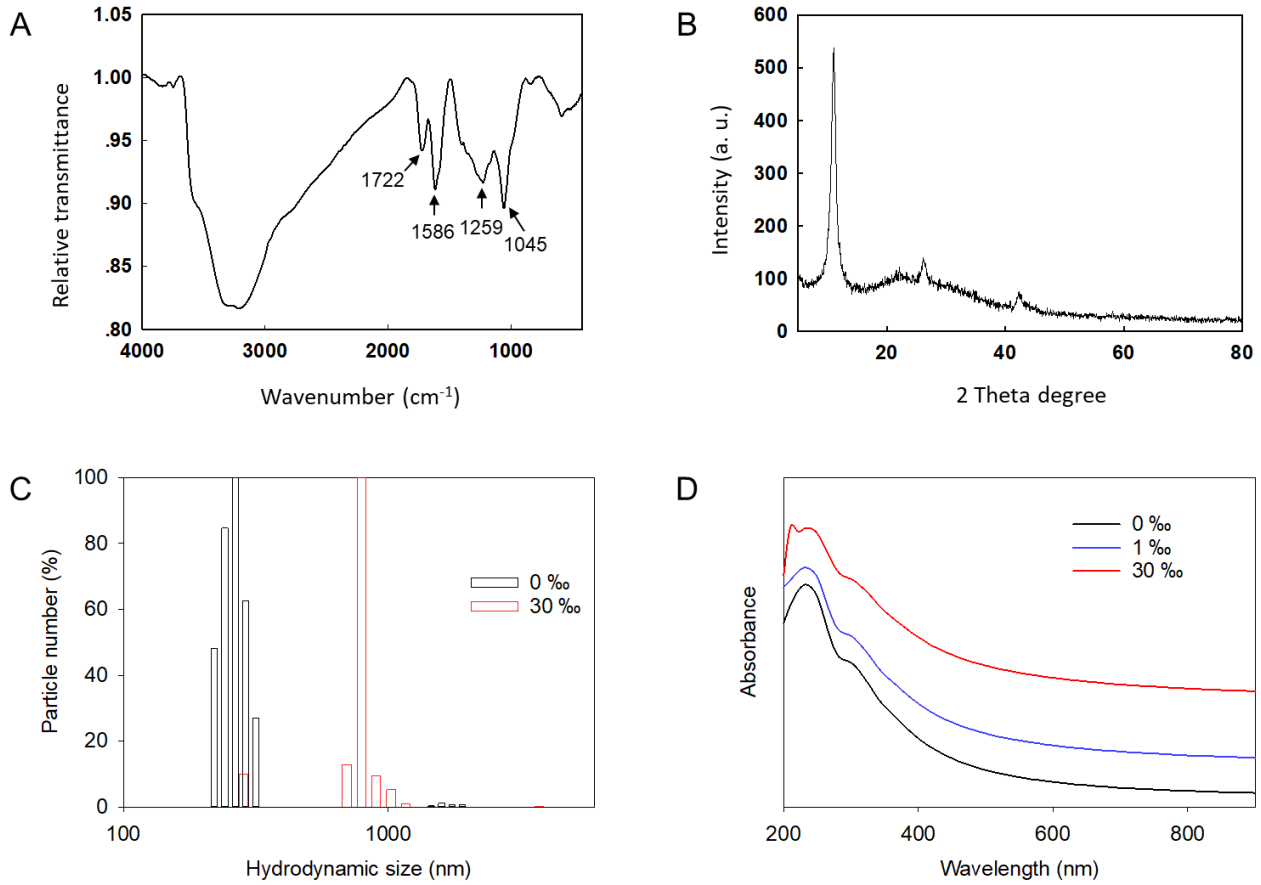


Figure S2. Characterization of the GO used in this study. (a) FTIR spectrum, and (b) X-ray diffraction (XRD) of pristine GO powder. (c) Number-based size distribution and (d) UV-Vis absorbance spectra of GO in aqueous media.

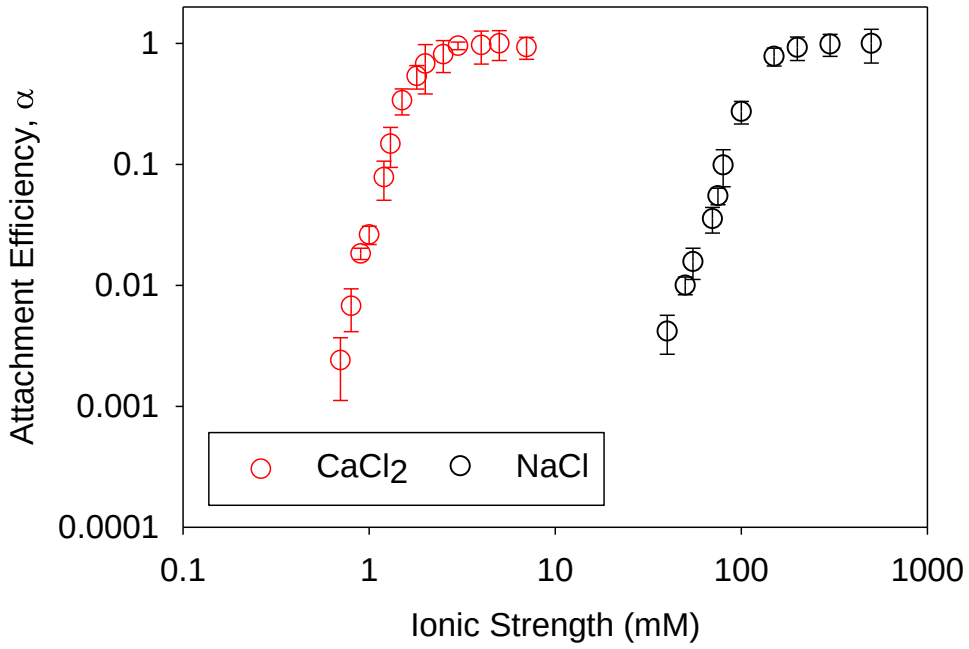


Figure S3. Impact of ionic strength on the attachment efficiency of GO in the presence of NaCl and $CaCl_2$. Critical coagulation concentration (CCC) values were determined as 138 mM NaCl and 1.73 mM $CaCl_2$.

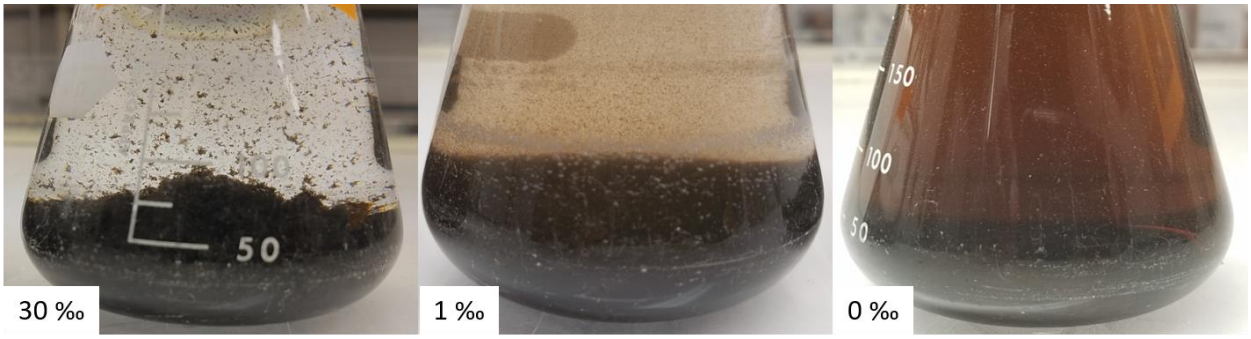


Figure S4. Images showing differences in the size and morphology of GO agglomerates formed at different water salinities.

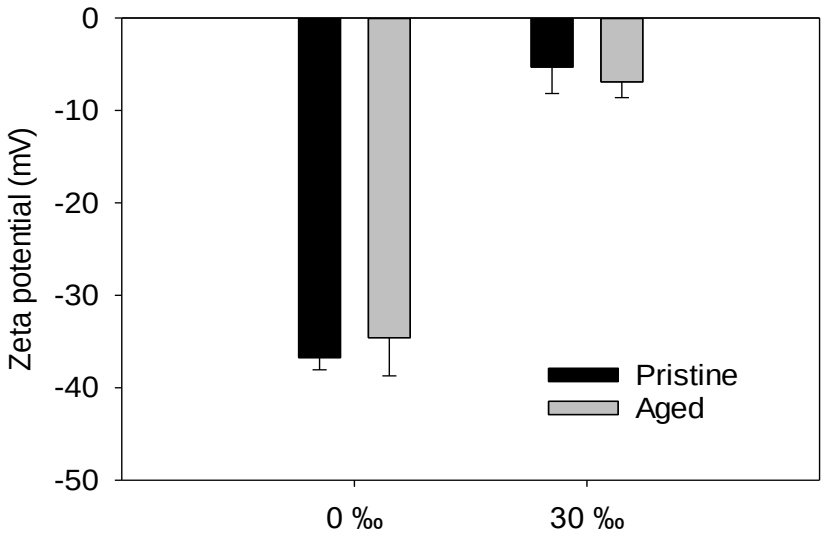


Figure S5. Zeta (ζ) potential of pristine and 28-d aged GO at 0 and 30 ‰.

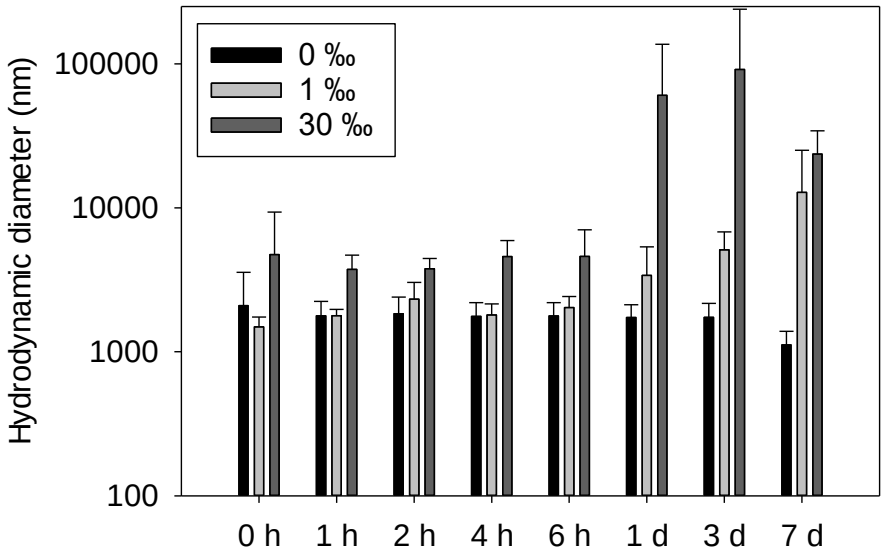


Figure S6. Hydrodynamic diameter of GO measured in media (0, 1, and 30 ‰) over 7 d. Note that the y-axis is log-scaled

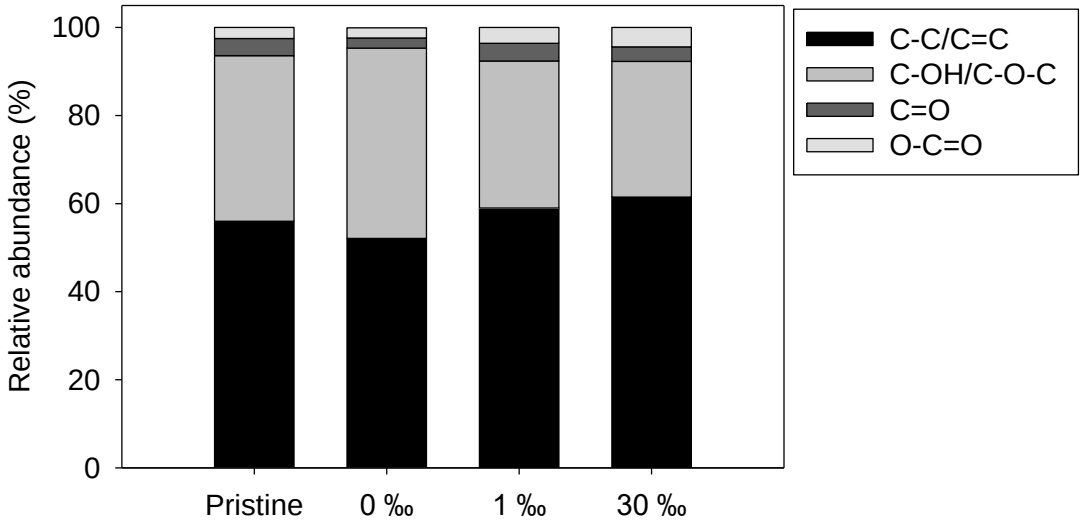


Figure S7. Relative abundance of different oxygen functional groups detected on the surface of pristine GO and GO aged for 28 days in 0, 1, and 30 ‰ media

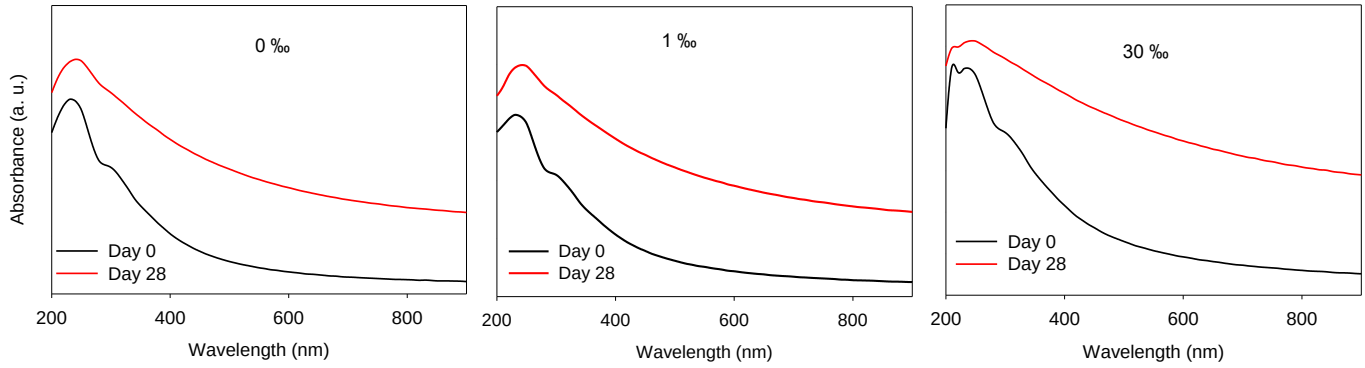


Figure S8. UV-Vis absorbance spectra of GO suspended in 0, 1, and 30 ‰ media on Day 0 and after aging for 28 days

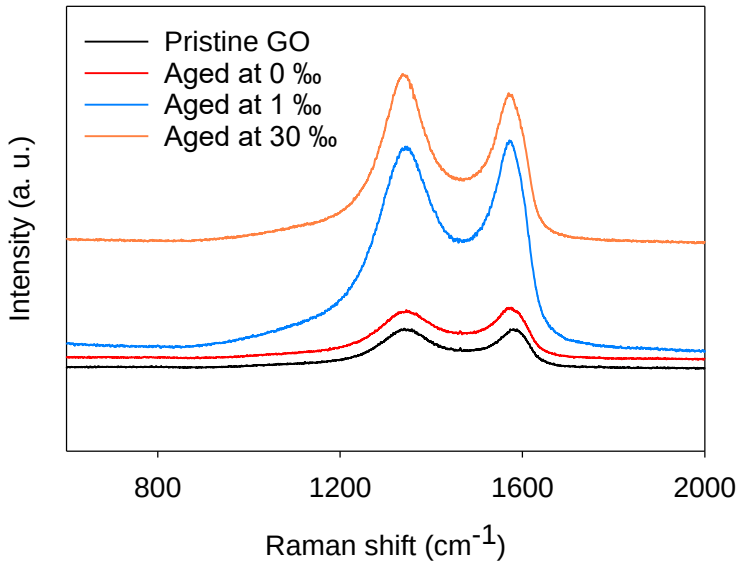


Figure S9. Raman spectra of pristine GO powder and aged suspensions of GO prepared in 0, 1, and 30 ‰. $I_D/I_G$ ratio of GO was 0.95, 0.97, and 1.13, in 0, 1, and 30 ‰ media, respectively

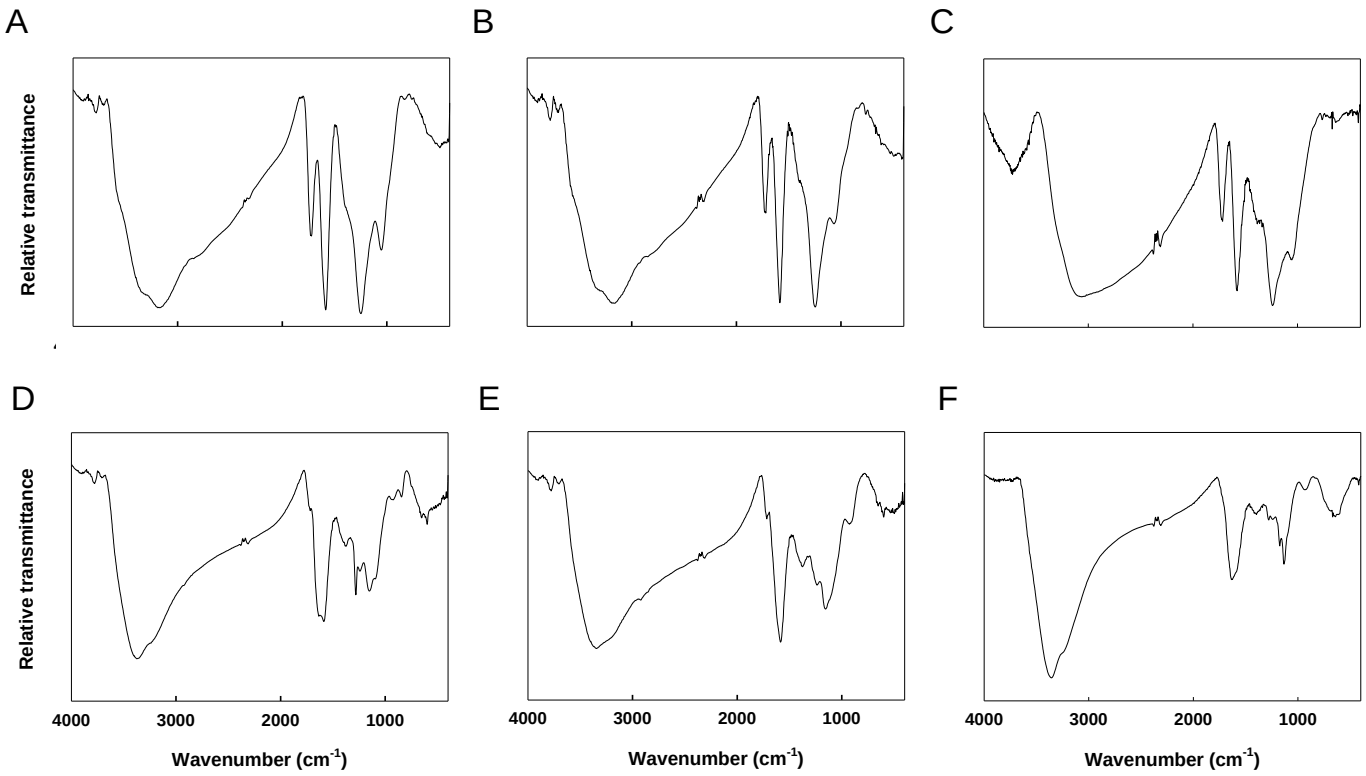


Figure S10. FTIR spectra of GO suspensions exposed to solar irradiation at 0 ‰ for (A) 6 h, (B) 12 h, and (C) 24 h; and at 30 ‰ for (D) 6 h, (E) 12 h, and (F) 24 h

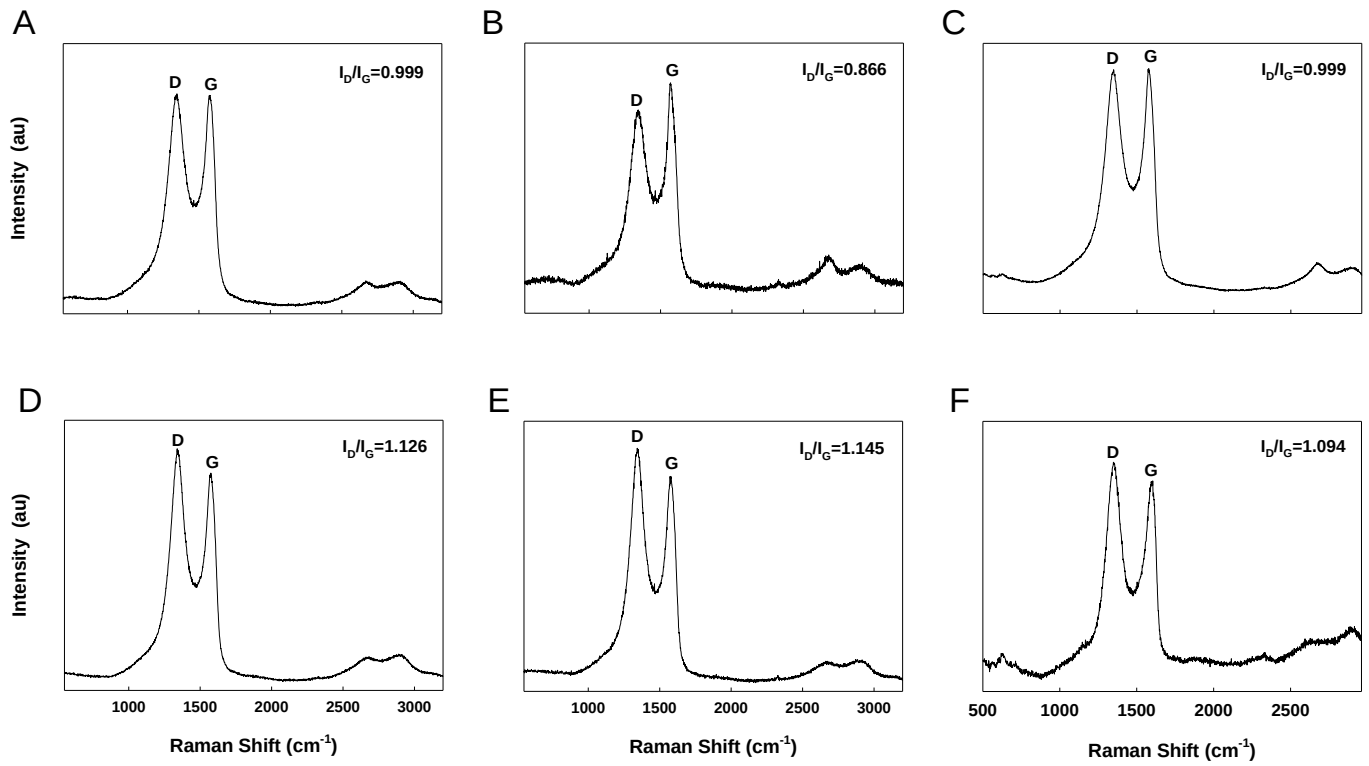


Figure S11. Raman spectra of GO suspensions exposed to solar irradiation at 0 ‰ for (A) 6 h, (B) 12 h, and (C) 24 h; and at 30 ‰ for (D) 6 h, (E) 12 h, and (F) 24 h

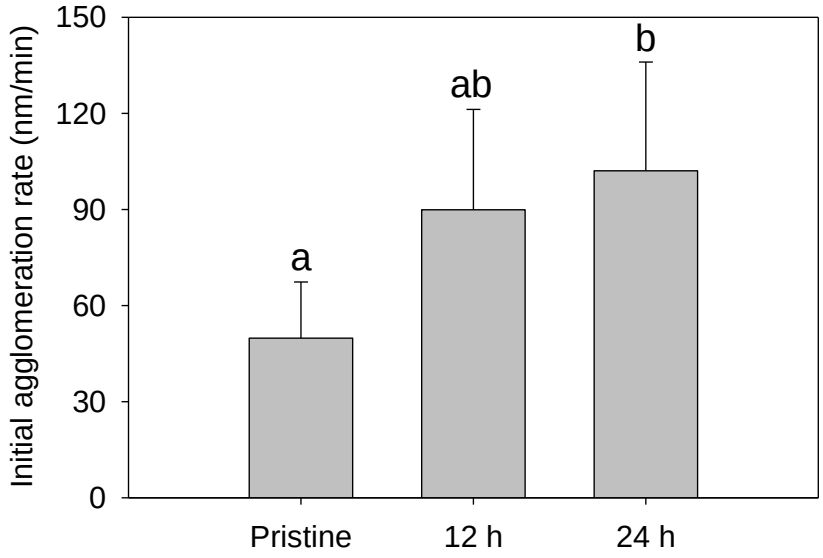


Figure S12. Initial agglomeration rate constants of pristine GO and GO treated with solar irradiation for 12 or 24 h

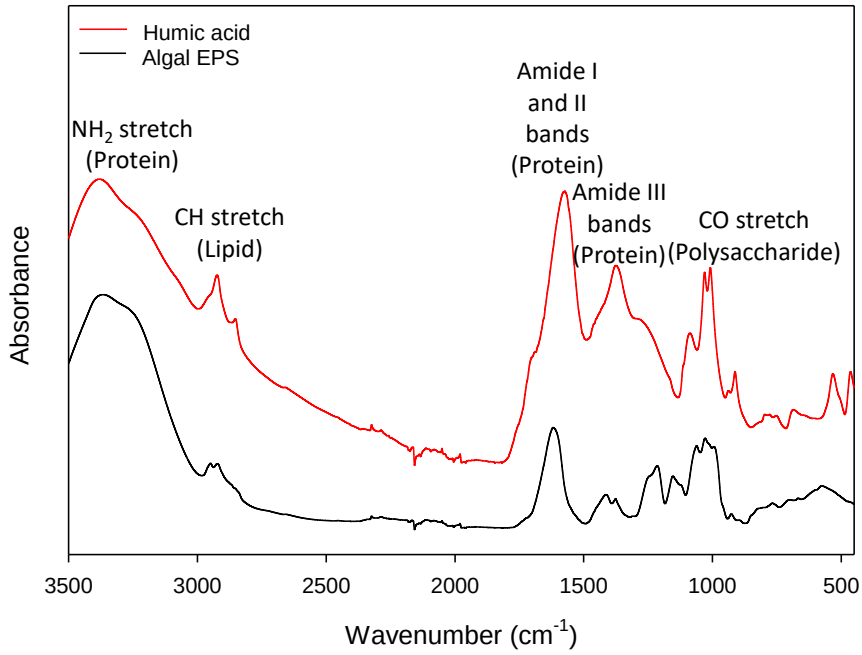


Figure S13. FTIR spectra of humic acid and algal extracellular polymeric substances (EPS) produced by *Tetraselmis* sp. Peak assignments are shown in Tables S1 and S2.

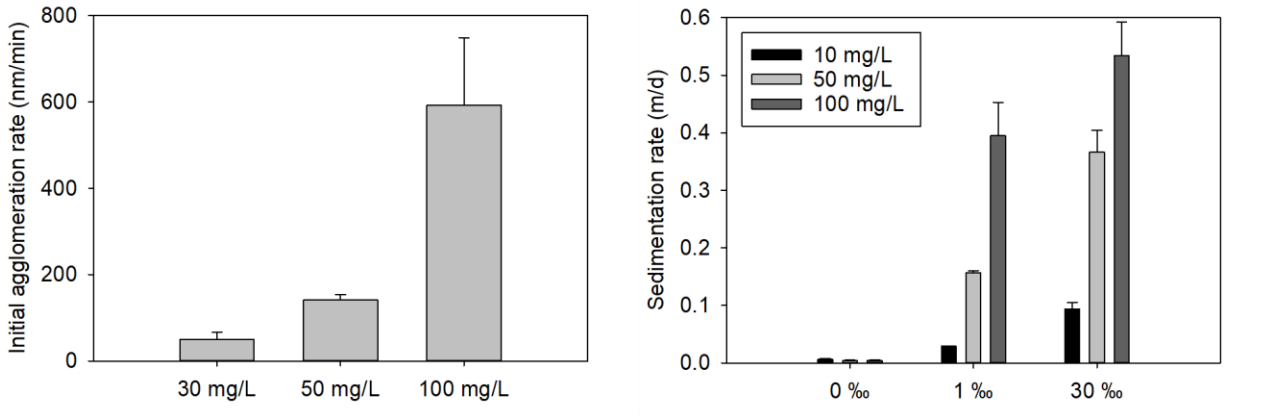


Figure 14. (a) Initial agglomeration constant of GO at an initial concentration of 30, 50, and 100 mg/L. (b) Sedimentation rate of GO at an initial concentration of 30, 50, and 100 mg/L in 0, 1, and 30 ‰ media.

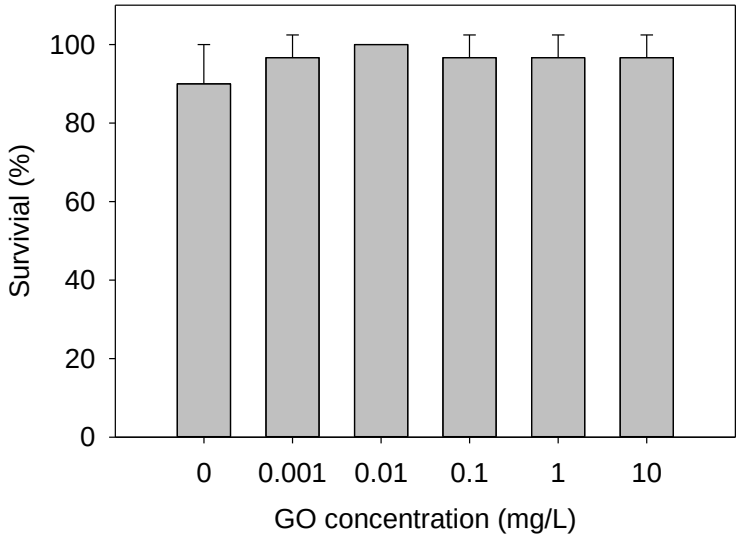


Figure S15. Survival of mysids (*Americamysis bahia*) exposed to GO (0-10 mg/L) at 30 ‰ for 96 h. Tests were conducted based on Ho *et al*. 2000.[13]

References


1. Adeleye, A. S.; Pokhrel, S.; Mädler, L.; Keller, A. A., Influence of nanoparticle doping on the colloidal stability and toxicity of copper oxide nanoparticles in synthetic and natural waters. *Water research* **2018,** *132*, 12-22.
2. Chowdhury, I.; Hou, W.-C.; Goodwin, D.; Henderson, M.; Zepp, R. G.; Bouchard, D., Sunlight affects aggregation and deposition of graphene oxide in the aquatic environment. *Water research* **2015,** *78*, 37-46.
3. Adeleye, A. S. Influence of Phytoplankton and Extracellular Polymeric Substances on the Fate of Engineered Nanomaterials in Natural Aquatic Systems. PhD Thesis, University of California, Santa Barbara, 2015.
4. Adeleye, A. S.; Keller, A. A., Interactions between Algal Extracellular Polymeric Substances and Commercial TiO2 Nanoparticles in Aqueous Media. *Environmental Science & Technology* **2016,** *50*, (22), 12258-12265.
5. Adeleye, A. S.; Keller, A. A., Long-term colloidal stability and metal leaching of single wall carbon nanotubes: effect of temperature and extracellular polymeric substances. *Water research* **2014,** *49*, (0), 236-50.
6. Goodwin, D. G., Jr.; Adeleye, A. S.; Sung, L.; Ho, K. T.; Burgess, R. M.; Petersen, E. J., Detection and Quantification of Graphene-Family Nanomaterials in the Environment. *Environmental Science & Technology* **2018,** *52*, (8), 4491-4513.
7. Goodwin, D.; Adeleye, A. S.; Sung, L.; Ho, K. T.; Burgess, R. M.; Petersen, E. J., Detection and Quantification of Graphene Family Nanomaterials in the Environment. *Environmental Science & Technology* **2018**.
8. Quik, J. T. K.; Velzeboer, I.; Wouterse, M.; Koelmans, A. A.; van de Meent, D., Heteroaggregation and sedimentation rates for nanomaterials in natural waters. *Water research* **2014,** *48*, 269-279.
9. Chowdhury, I.; Duch, M. C.; Mansukhani, N. D.; Hersam, M. C.; Bouchard, D., Colloidal Properties and Stability of Graphene Oxide Nanomaterials in the Aquatic Environment. *Environmental Science & Technology* **2013,** *47*, (12), 6288-6296.
10. Badireddy, A. R.; Chellam, S.; Gassman, P. L.; Engelhard, M. H.; Lea, A. S.; Rosso, K. M., Role of extracellular polymeric substances in bioflocculation of activated sludge microorganisms under glucose-controlled conditions. *Water research* **2010,** *44*, (15), 4505-4516.
11. Zhu, L.; Qi, H.-y.; Lv, M.-l.; Kong, Y.; Yu, Y.-w.; Xu, X.-y., Component analysis of extracellular polymeric substances (EPS) during aerobic sludge granulation using FTIR and 3D-EEM technologies. *Bioresource Technology* **2012,** *124*, 455-459.
12. Omoike, A.; Chorover, J., Spectroscopic Study of Extracellular Polymeric Substances from Bacillus subtilis: Aqueous Chemistry and Adsorption Effects. *Biomacromolecules* **2004,** *5*, (4), 1219-1230.
13. Ho, K. T.; Kuhn, A.; Pelletier, M.; McGee, F.; Burgess, R. M.; Serbst, J. J. A. o. E. C.; Toxicology, Sediment Toxicity Assessment: Comparison of Standard and New Testing Designs. **2000,** *39*, (4), 462-468.